

# Spaatind 2020

## Lecture 2 Gravitational Waves: Astrophysics

Alex Nielsen  
University of Stavanger

# TOPICS

1) **What are gravitational waves?**

Theoretical background

2) **How do we know we are seeing gravitational waves?**

Detecting new signals

3) **What can we use gravitational waves for?**

Astrophysics with gravitational waves

Fundamental physics with gravitational waves

# Masses in the Stellar Graveyard

*in Solar Masses*

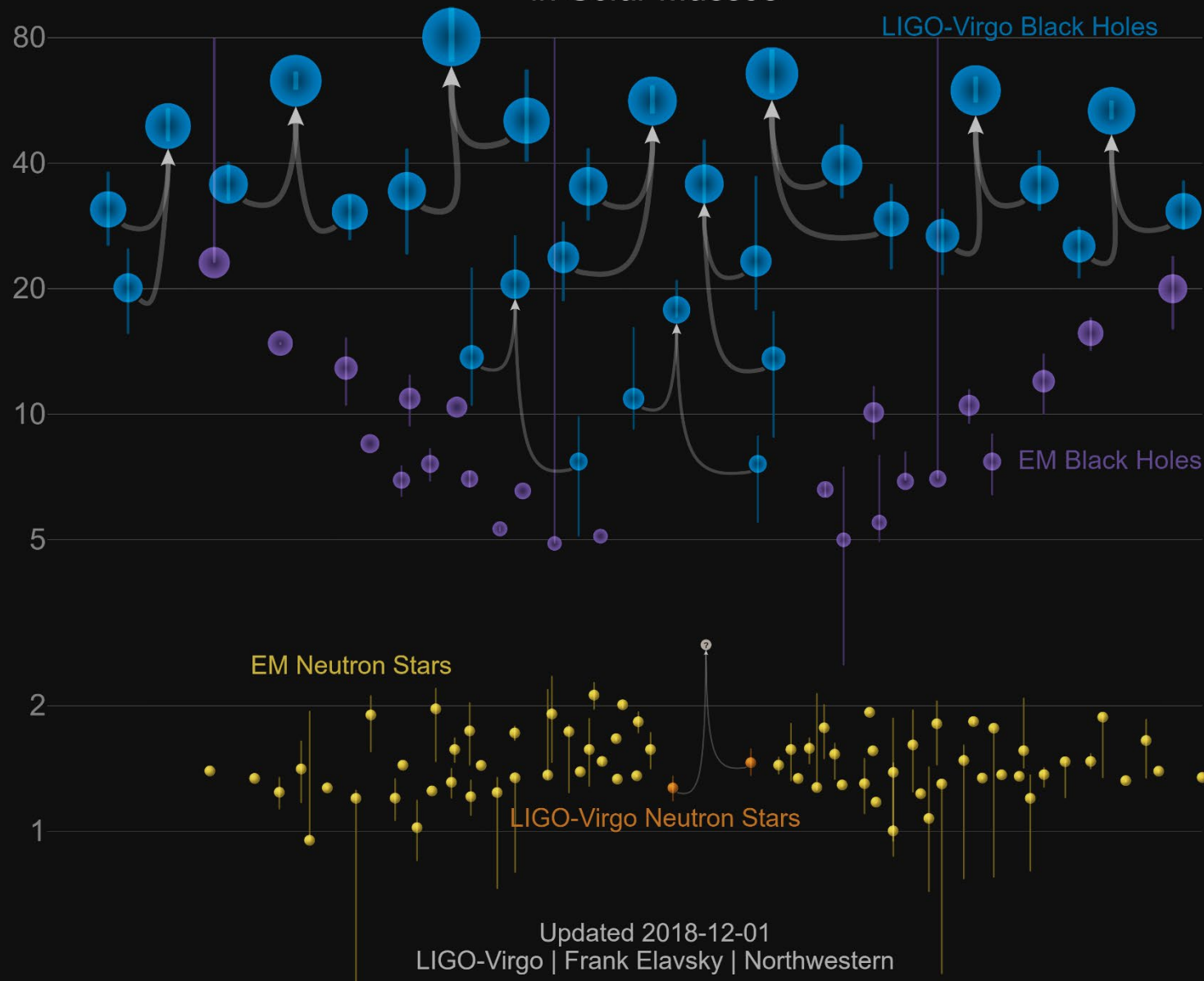


[Image credit: LIGO-Virgo/Frank Elavsky/Northwestern University]

# Detection statistics

- **Task:** Separate data  $x$  into signals and noise
- **Approach:** Compute some statistic  $f(x)$  and compare to a threshold  $T$ .
- Neyman-Pearson criterion: maximise  $p_{\text{Detection}}$  at fixed  $p_{\text{False alarm}}$
- **Solution:** compute a likelihood ratio

$$f(x) = \frac{p(x|H_{\text{signal}})}{p(x|H_{\text{noise}})} > T$$

# Bayesian interpretation

$$\frac{p(H_{signal}|x)}{p(H_{noise}|x)} = \frac{p(x|H_{signal})}{p(x|H_{noise})} \frac{p(H_{signal})}{p(H_{noise})}$$

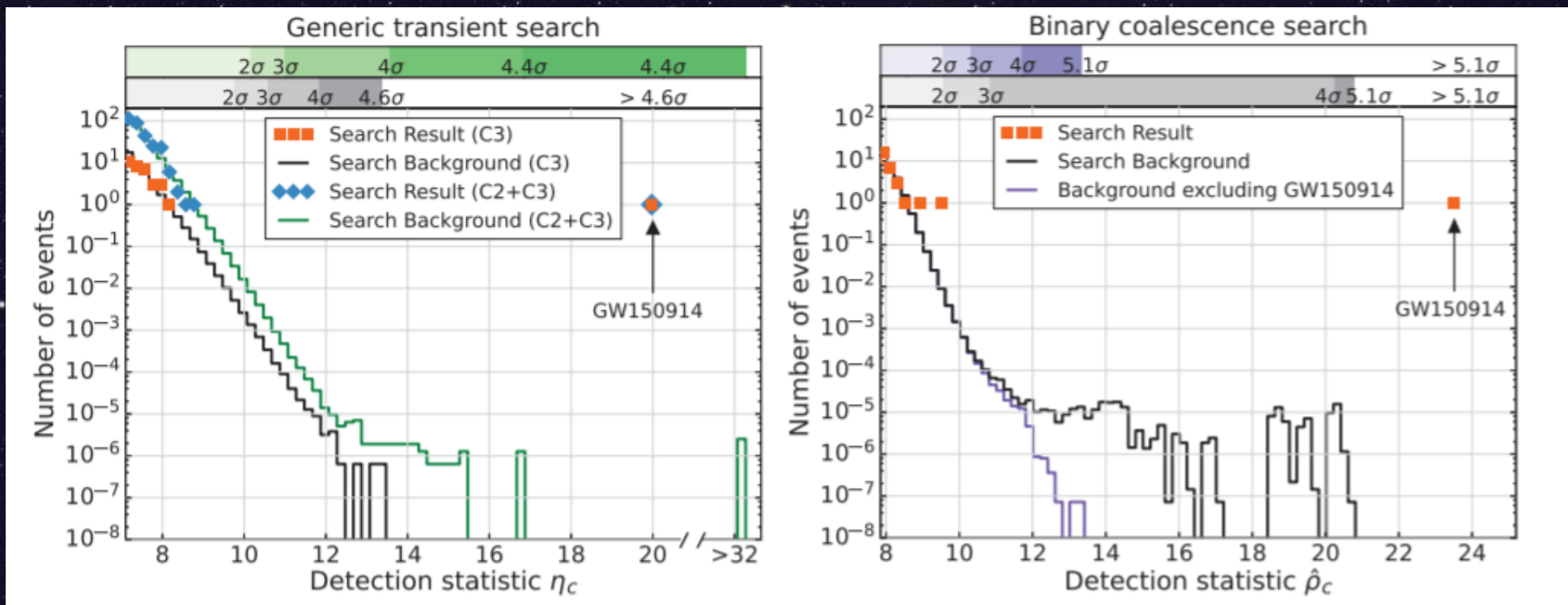
$$p(x|H_{signal}) = \int p(x|\sigma, H_{signal})p(\sigma)d\sigma$$

*Monte-Carlo simulation parameter distribution  
corresponds to prior parameter distribution*

# Limitations in real life

- Need a parameterised noise model
- GW detectors: cannot turn off signal
- Need a parameterised signal model
- GW detectors: cannot turn on signal
- For large parameter spaces, marginalisation may be expensive
- Result will depend on prior distributions

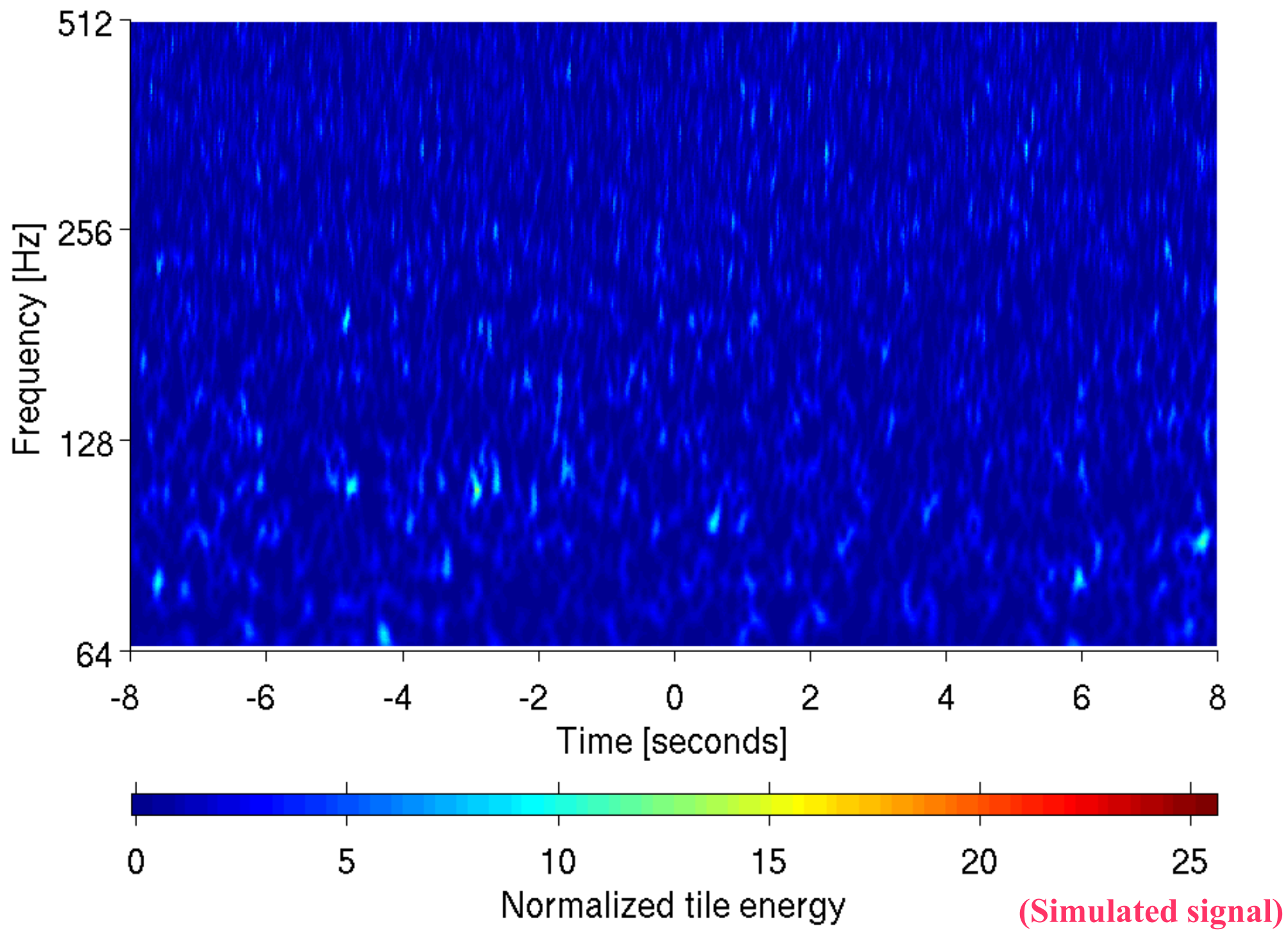
Fig 4 of LVC, PRL116 (2016) 061102



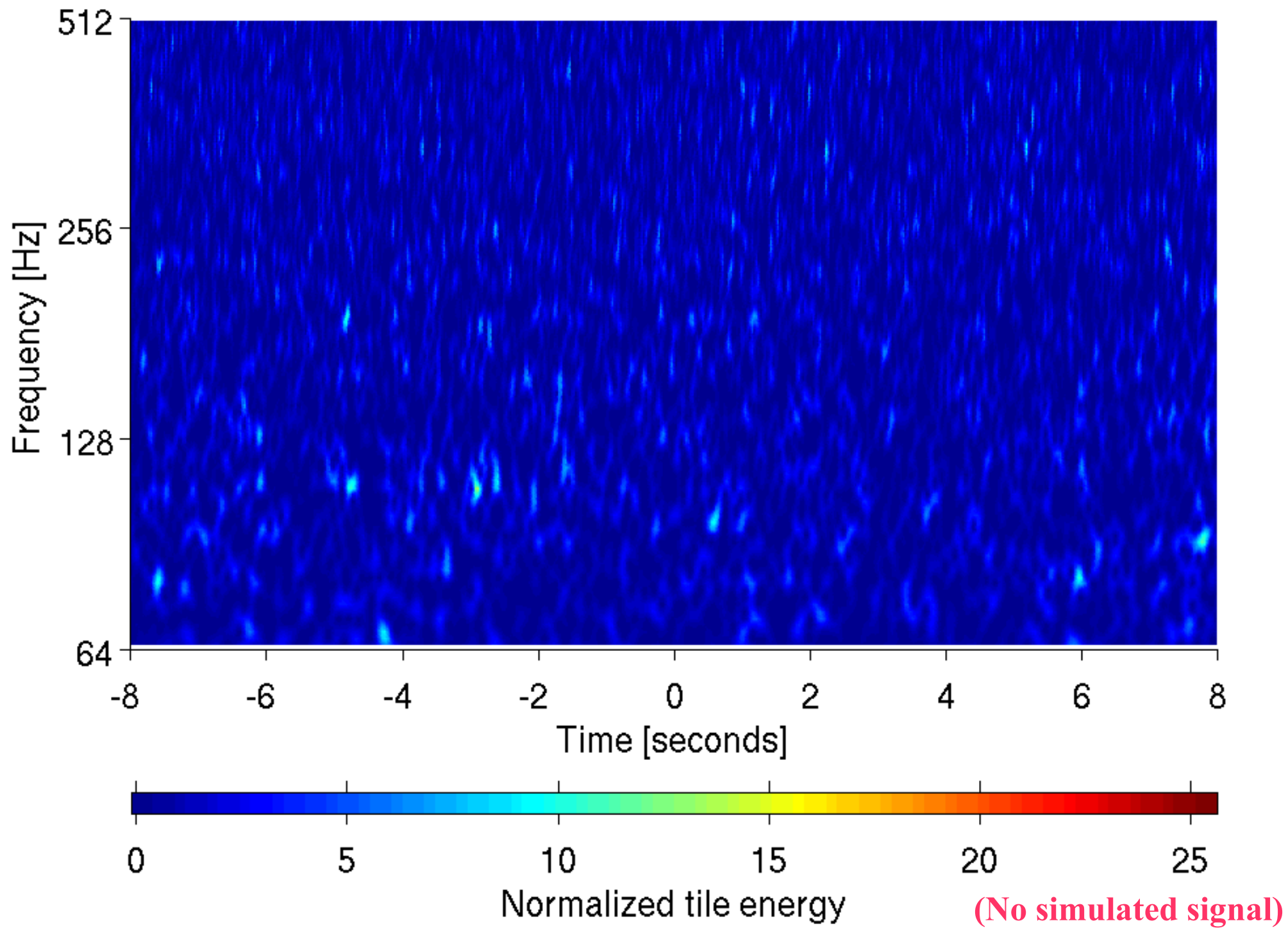
Unmodeled, coherent  
power search

Modeled, template-based  
matched filter search

Channel 1 at 932451272.000 with Q of 45.3



Channel 1 at 932451272.000 with Q of 45.3



# Gravitational Waveforms

- **Numerical relativity**

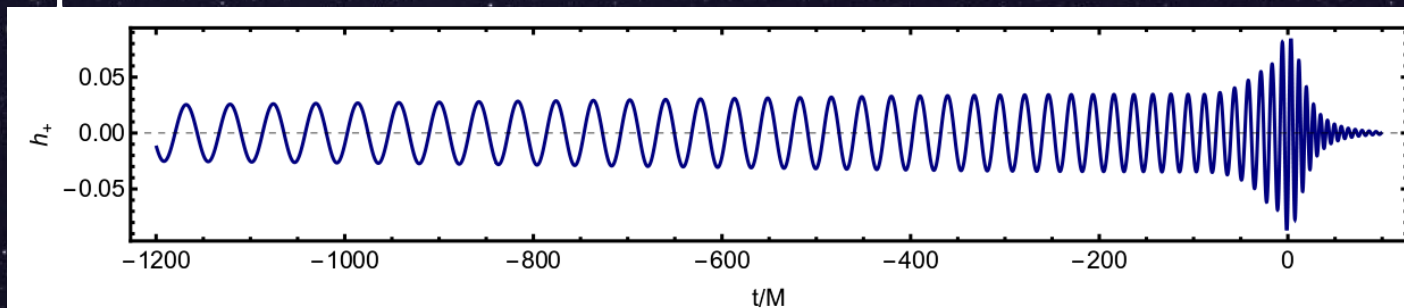
either finite differencing or spectral methods

- **Effective One Body (EOBNR)**

maps two body problem to one body problem via effective Hamiltonian  
and calibrated to numerical simulations

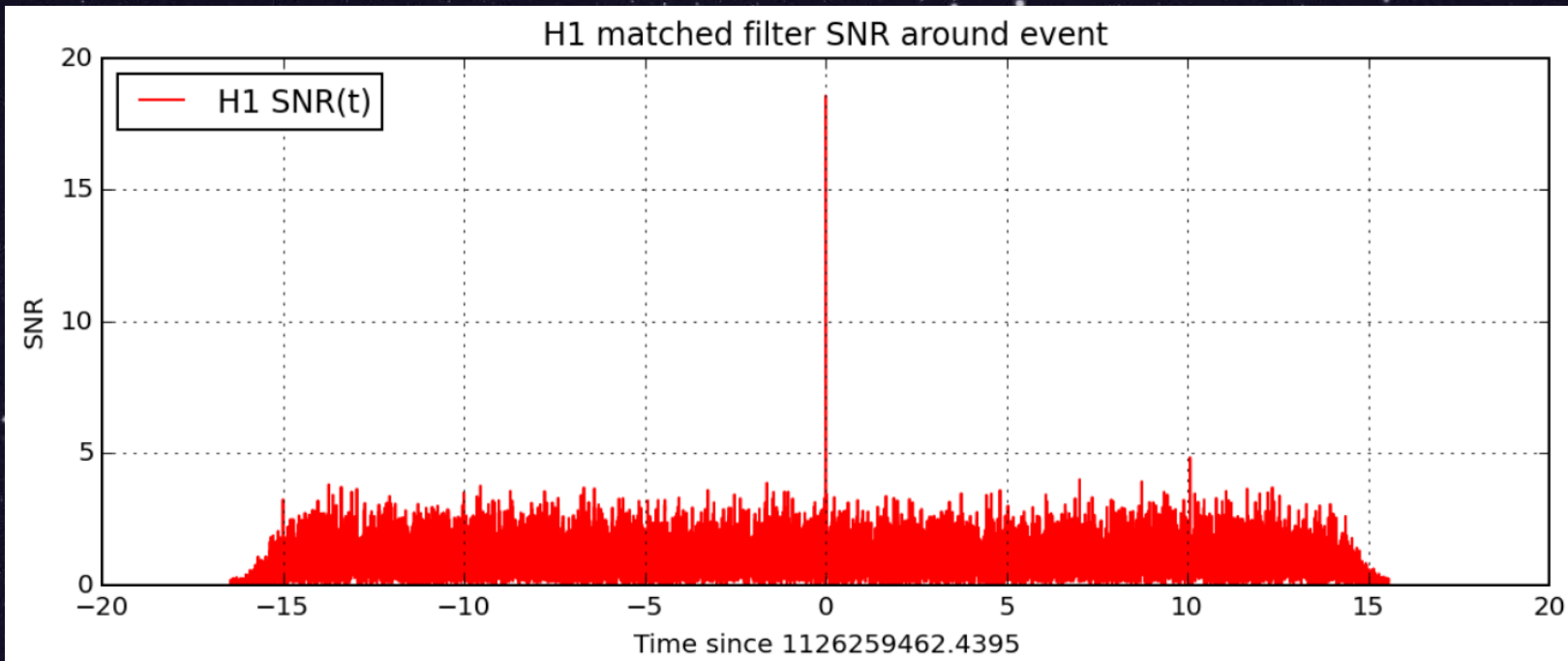
- **IMRPhenom**

combines post-Newtonian inspiral with phenomenological fit model of  
numerical simulations of late inspiral and merger, and quasi-analytical  
ringdown phase

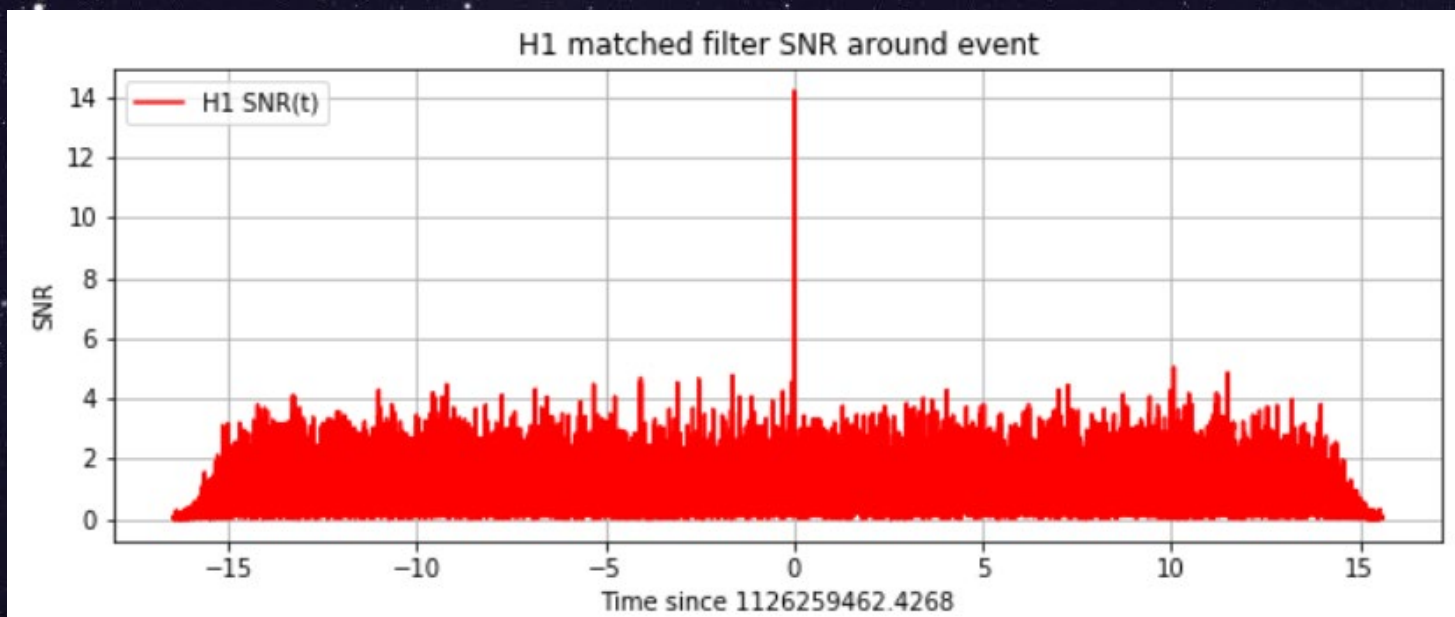


# Post-Newtonian expansion (2-2 phase)

| PN order | Includes<br>(amongst other things)   |
|----------|--|
| 0PN      | Kepler<br>Newtonian Gravity  |
| 0.5PN    | Zero in GR   |
| 1PN      | Pericenter advance (cf zero)<br>PPN parameters   |
| 1.5PN    | Spin-orbit couplings<br>Gravitational tails (backscatter)  |
| 2PN      | Spin-spin couplings<br>(Newtonian) quadrupole-monopole (GR BH)<br>(Newtonian) magnetic dipole-dipole (cf zero) |
| 3PN      | Tails of tails   |
| 5PN      | (Newtonian) Adiabatic tidal deformations   |



*SEOBNRv2 source: <https://www.gw-openscience.org>*



*OPN figure courtesy Madhu Jha*

# Post-Newtonian phase bounds

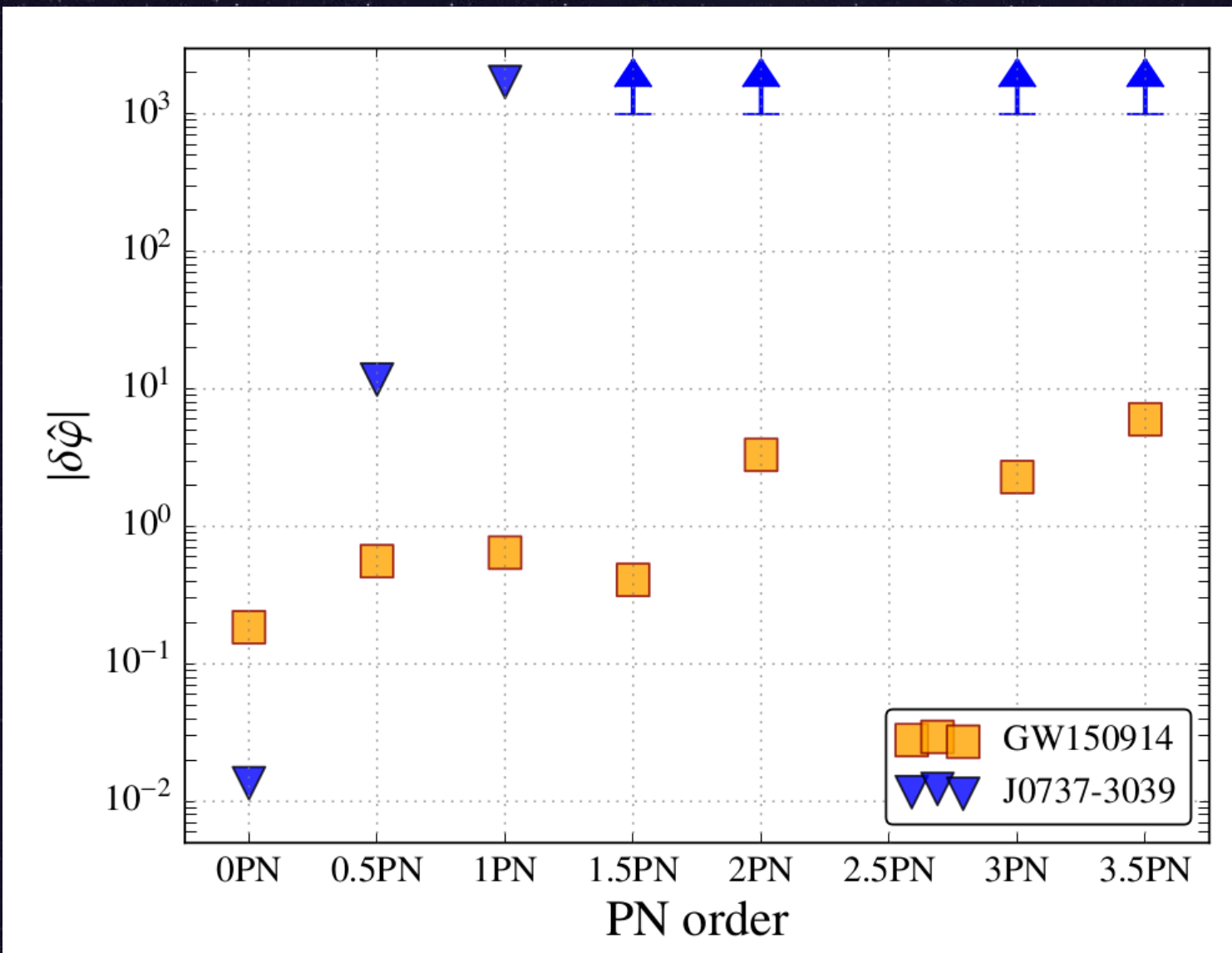


Fig. 6 of LVC PRL 16 (2016) 221101

# Theoretical rates: predictions becoming constraints

TABLE II: Compact binary coalescence rates per Milky Way Equivalent Galaxy per Myr.

| Source   | $R_{\text{low}}$       | $R_{\text{re}}$       | $R_{\text{high}}$       | $R_{\text{max}}$       |
|--|------------------------|-----------------------|-------------------------|------------------------|
| NS-NS ( $\text{MWEG}^{-1} \text{ Myr}^{-1}$ )        | 1 [1] <sup>a</sup>     | 100 [1] <sup>b</sup>  | 1000 [1] <sup>c</sup>   | 4000 [16] <sup>d</sup> |
| NS-BH ( $\text{MWEG}^{-1} \text{ Myr}^{-1}$ )        | 0.05 [18] <sup>e</sup> | 3 [18] <sup>f</sup>   | 100 [18] <sup>g</sup>   |                        |
| BH-BH ( $\text{MWEG}^{-1} \text{ Myr}^{-1}$ )        | 0.01 [14] <sup>h</sup> | 0.4 [14] <sup>i</sup> | 30 [14] <sup>j</sup>    |                        |
| IMRI into IMBH ( $\text{GC}^{-1} \text{ Gyr}^{-1}$ ) |                        |                       | 3 [19] <sup>k</sup>     | 20 [19] <sup>l</sup>   |
| IMBH-IMBH ( $\text{GC}^{-1} \text{ Gyr}^{-1}$ )      |                        |                       | 0.007 [20] <sup>m</sup> | 0.07 [20] <sup>n</sup> |

<sup>a</sup>Lower end of 95% confidence interval for the pulsar luminosity distribution yielding the lowest rate (Model 14) in Table 1 of [1]

<sup>b</sup>Peak rate for the reference pulsar luminosity distribution (Model 6) in Table 1 of [1]

<sup>c</sup>Upper end of 95% confidence interval for the pulsar luminosity distribution yielding the highest rate (Model 15) in Table 1 of [1]

<sup>d</sup>Mean rates plus  $2\sigma$  for Type Ib/Ic supernova [16], values from [17]

<sup>e</sup>The left edge of the probability distribution peak for NS-BH in Figure 6 of [18]

<sup>f</sup>The center of the probability distribution peak for NS-BH in Figure 6 of [18]

<sup>g</sup>The right edge of the probability distribution peak for NS-BH in Figure 6 of [18]

<sup>h</sup>The left edge of the probability distribution peak for BH-BH in Figure 15 of [14]

<sup>i</sup>The center of the probability distribution peak for BH-BH in Figure 15 of [14]

<sup>j</sup>The right edge of the probability distribution peak for BH-BH in Figure 15 of [14]

<sup>k</sup>Estimate from binary hardening via three-body interactions assuming the inspiraling object is a neutron star (Section 2.1 of [19])

<sup>l</sup>Upper limit of  $300M_{\odot}/m$  per  $10^{10}$  years per cluster (Section 3.3 of [19]), assuming the inspiraling object  $m = 1.4 M_{\odot}$  is a neutron star

<sup>m</sup>Assumes that 10% of all globular clusters are sufficiently massive and have a sufficient binary fraction to form an IMBH-IMBH binary once in their lifetime, taken to be 13.8 Gyr [20]

<sup>n</sup>Assumes that all globular clusters are sufficiently massive and have a sufficient binary fraction to form an IMBH-IMBH binary once in their lifetime, taken to be 13.8 Gyr [20]

# Data-fitted noise and signal models after O1

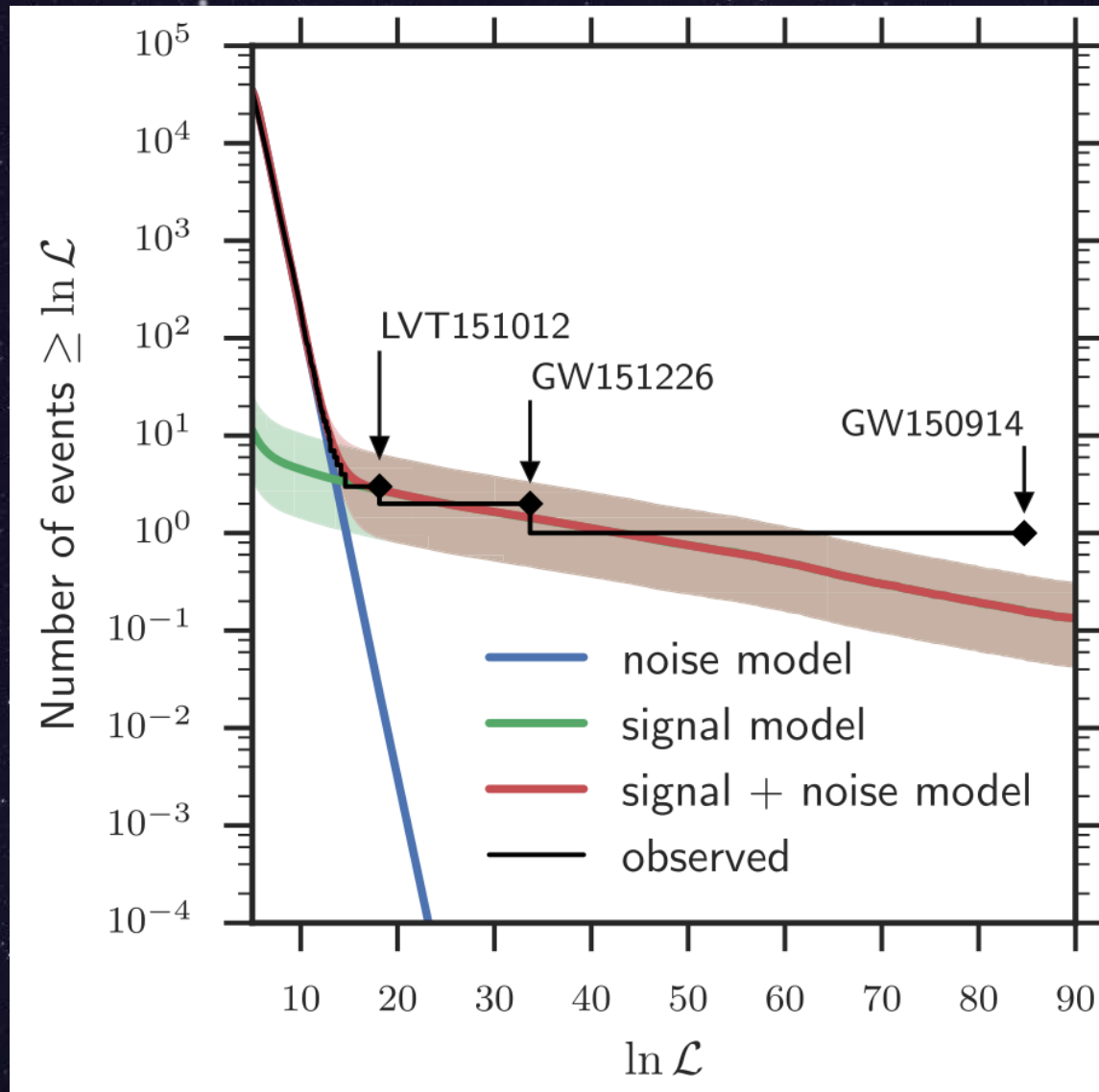


Fig 9 of LVC 1606.04856 PRX6 041015

# New signals, 2-OGC catalogue

| Date designation   | GPS time      | $p_{\text{astro}}$ | FAR $^{-1}$ (y)   | Det. | $\tilde{\Lambda}_{\text{BBH}}$ | $\rho_H$ | $\rho_L$ | $\rho_V$ | $m_1^{\text{src}}$    | $m_2^{\text{src}}$    | $\chi_{\text{eff}}$       | $D_L$ (Mpc)            |
|--------------------|---------------|--------------------|-------------------|------|--------------------------------|----------|----------|----------|-----------------------|-----------------------|---------------------------|------------------------|
| 150914+09:50:45UTC | 1126259462.43 | > 0.999            | > 10000           | HL   | 111.71                         | 19.7     | 13.4     | -        | $35.4^{+5.3}_{-3.2}$  | $29.8^{+3.1}_{-4.7}$  | $-0.04^{+0.11}_{-0.13}$   | $470^{+140}_{-190}$    |
| 170814+10:30:43UTC | 1186741861.53 | > 0.999            | > 10000           | HL   | 61.58                          | 9.3      | 13.8     | -        | $30.4^{+5.6}_{-2.7}$  | $25.8^{+2.6}_{-4}$    | $0.08^{+0.12}_{-0.12}$    | $580^{+130}_{-190}$    |
| 170823+13:13:58UTC | 1187529256.52 | > 0.999            | > 10000           | HL   | 59.43                          | 6.3      | 9.2      | -        | $40^{+11.7}_{-7.1}$   | $28.8^{+6.8}_{-7.9}$  | $0.05^{+0.21}_{-0.22}$    | $1750^{+850}_{-820}$   |
| 170104+10:11:58UTC | 1167559936.60 | > 0.999            | > 10000           | HL   | 47.32                          | 9.1      | 9.9      | -        | $31.6^{+7.8}_{-6.3}$  | $19.2^{+5}_{-4.1}$    | $-0.08^{+0.16}_{-0.18}$   | $920^{+420}_{-400}$    |
| 151226+03:38:53UTC | 1135136350.65 | > 0.999            | > 10000           | HL   | 40.58                          | 10.7     | 7.4      | -        | $13.9^{+7.9}_{-3.3}$  | $7.6^{+2.2}_{-2.3}$   | $0.209^{+0.177}_{-0.077}$ | $460^{+160}_{-180}$    |
| 151012+09:54:43UTC | 1128678900.45 | > 0.999            | > 10000           | HL   | 20.25                          | 7.0      | 6.7      | -        | $22.4^{+13.4}_{-4.8}$ | $13.8^{+3.7}_{-4.8}$  | $-0.00^{+0.25}_{-0.16}$   | $990^{+470}_{-460}$    |
| 170809+08:28:21UTC | 1186302519.76 | > 0.999            | 8300 <sup>a</sup> | HL   | 43.34                          | 6.6      | 10.7     | -        | $35.2^{+9.5}_{-5.9}$  | $23.9^{+5.1}_{-5.3}$  | $0.06^{+0.18}_{-0.16}$    | $980^{+310}_{-390}$    |
| 170729+18:56:29UTC | 1185389807.33 | > 0.999            | 4000              | HL   | 19.16                          | 7.5      | 7.1      | -        | $55^{+18}_{-13}$      | $32^{+13}_{-10}$      | $0.31^{+0.22}_{-0.29}$    | $2300^{+1600}_{-1300}$ |
| 170608+02:01:16UTC | 1180922494.49 | > 0.999            | > 910             | HL   | 55.12                          | 12.5     | 8.7      | -        | $11.6^{+6.7}_{-2.1}$  | $7.4^{+1.6}_{-2.3}$   | $0.088^{+0.213}_{-0.073}$ | $310^{+130}_{-110}$    |
| 170121+21:25:36UTC | 1169069154.58 | > 0.999            | 210 <sup>a</sup>  | HL   | 23.86                          | 5.1      | 8.9      | -        | $33^{+9.2}_{-5.3}$    | $25.7^{+5.3}_{-6.1}$  | $-0.17^{+0.24}_{-0.26}$   | $1150^{+950}_{-650}$   |
| 170818+02:25:09UTC | 1187058327.09 | > 0.999            | 5.1 <sup>a</sup>  | HL   | 21.42                          | 4.4      | 9.4      | -        | $36^{+8.2}_{-5.3}$    | $26.2^{+4.8}_{-5.7}$  | $-0.11^{+0.20}_{-0.23}$   | $980^{+430}_{-340}$    |
| 170727+01:04:30UTC | 1185152688.03 | 0.994              | 180               | HL   | 15.84                          | 4.5      | 6.9      | -        | $41.6^{+12.8}_{-7.9}$ | $30.4^{+7.9}_{-8.2}$  | $-0.05^{+0.25}_{-0.30}$   | $2200^{+1500}_{-1100}$ |
| 170304+16:37:53UTC | 1172680691.37 | 0.70               | 2.5               | HL   | 11.61                          | 4.6      | 7.1      | -        | $44.9^{+17.6}_{-9.4}$ | $31.8^{+9.5}_{-11.6}$ | $0.11^{+0.29}_{-0.27}$    | $2300^{+1600}_{-1200}$ |
| 151205+19:55:25UTC | 1133380542.42 | 0.53               | .61               | HL   | 10.97                          | 5.8      | 4.8      | -        | $67^{+28}_{-17}$      | $42^{+16}_{-19}$      | $0.14^{+0.40}_{-0.38}$    | $3000^{+2400}_{-1600}$ |
| 151217+03:47:49UTC | 1134359286.35 | 0.26               | .15               | HL   | 9.61                           | 6.7      | 5.6      | -        | $46^{+13}_{-26}$      | $8.2^{+5.1}_{-1.7}$   | $0.70^{+0.15}_{-0.50}$    | $1000^{+660}_{-440}$   |
| 170201+11:03:12UTC | 1169982210.74 | 0.24               | .16               | HL   | 9.26                           | 6.0      | 5.6      | -        | $48^{+13}_{-23}$      | $13.1^{+8.6}_{-3.7}$  | $0.44^{+0.28}_{-0.54}$    | $1530^{+1360}_{-770}$  |
| 170425+05:53:34UTC | 1177134832.19 | 0.21               | .2                | HL   | 9.42                           | 5.1      | 5.8      | -        | $45^{+21}_{-11}$      | $30^{+11}_{-11}$      | $-0.06^{+0.28}_{-0.32}$   | $2600^{+2000}_{-1300}$ |
| 151216+09:24:16UTC | 1134293073.19 | 0.18               | .1                | HL   | 9.25                           | 5.9      | 5.5      | -        | $41^{+15}_{-17}$      | $14.4^{+7}_{-6.3}$    | $0.51^{+0.21}_{-0.57}$    | $1620^{+1140}_{-910}$  |
| 170202+13:56:57UTC | 1170079035.73 | 0.13               | .06               | HL   | 8.37                           | 5.0      | 6.6      | -        | $33^{+17}_{-11}$      | $13.8^{+7}_{-4.8}$    | $-0.06^{+0.27}_{-0.32}$   | $1220^{+980}_{-640}$   |

Table 3 of Nitz et al, arXiv 1910.05331

# Binary Neutron Star GW170817

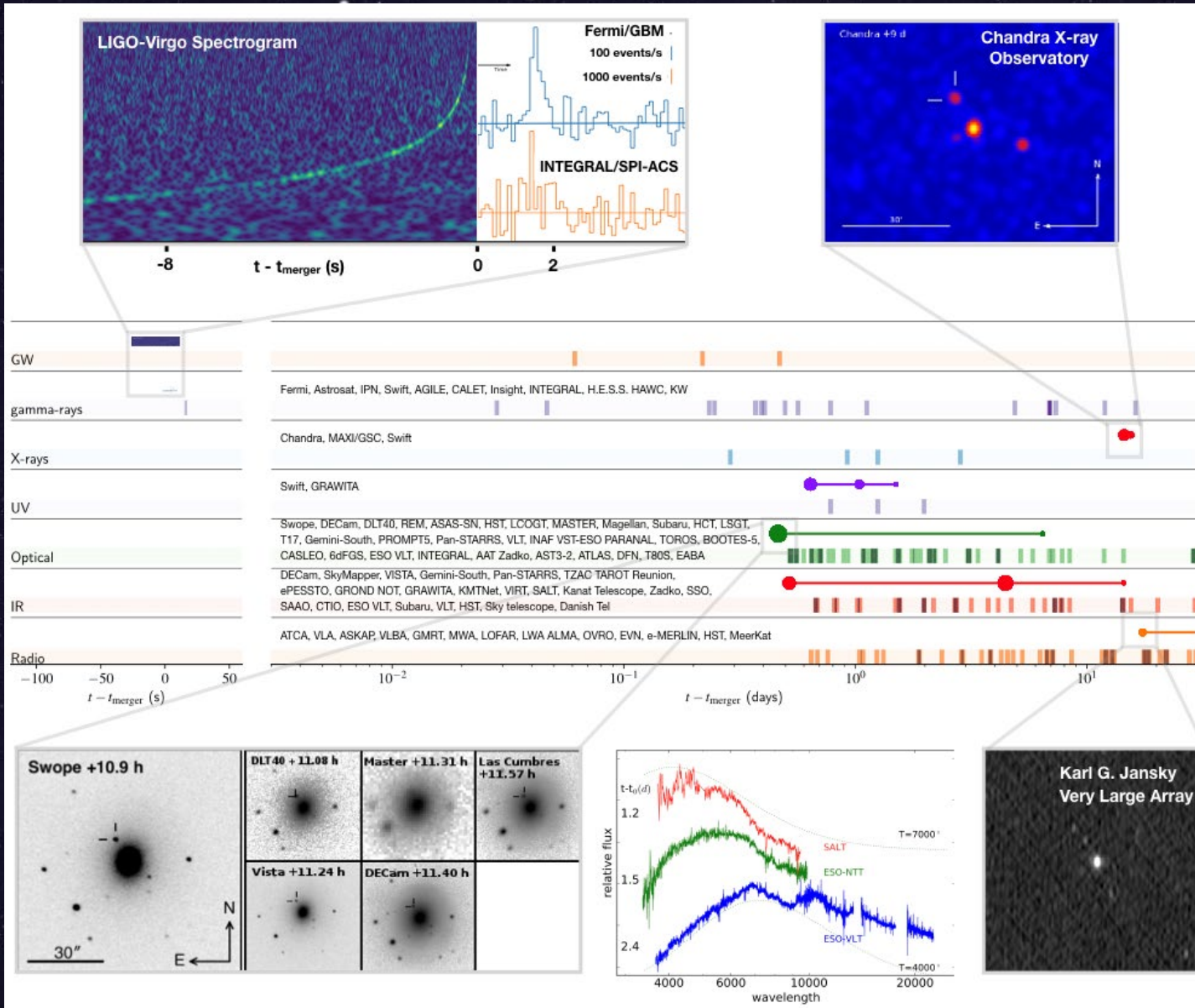


Fig 2, ApJL848, (2017) L12

# GW170817 sky location

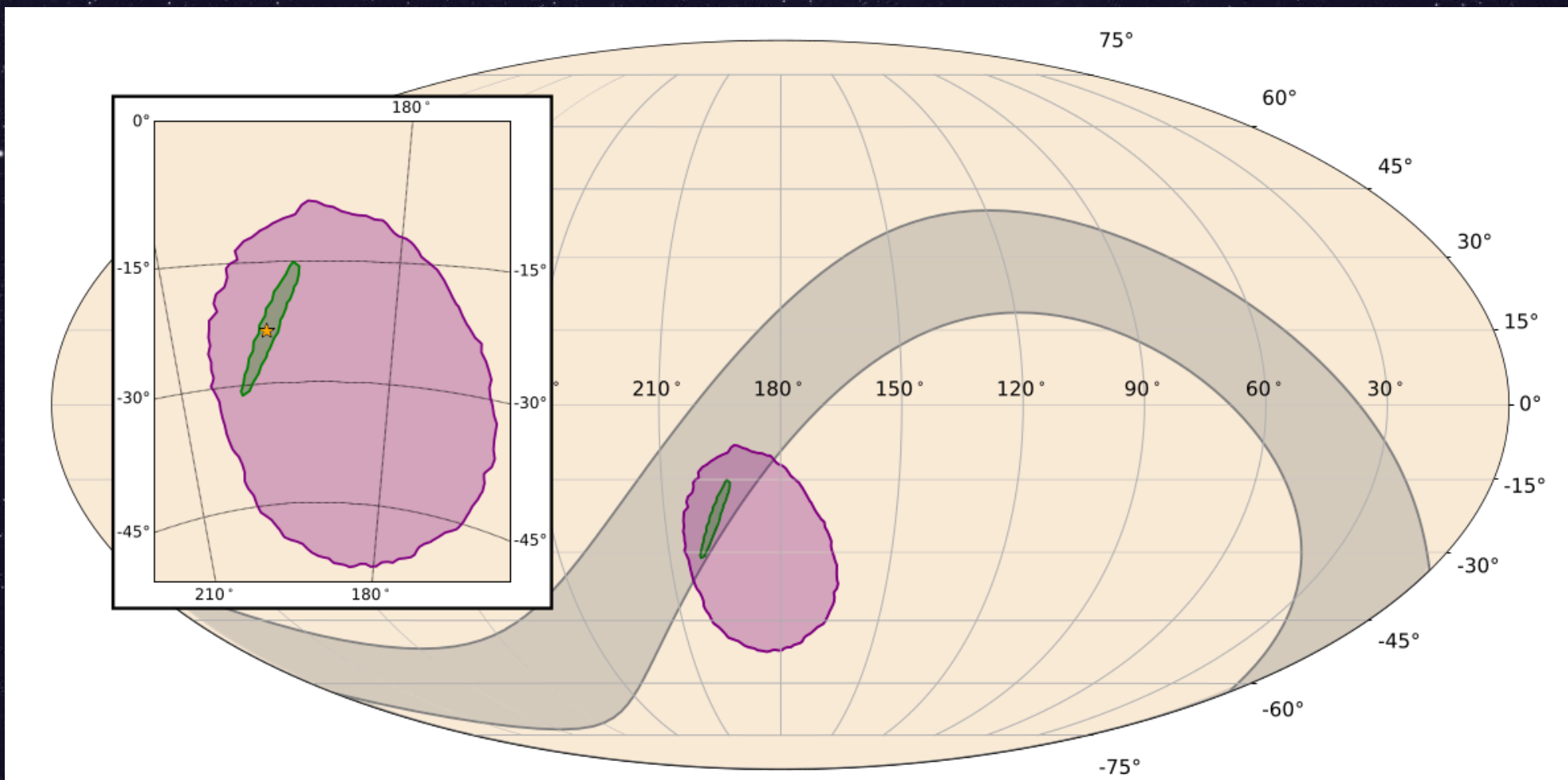
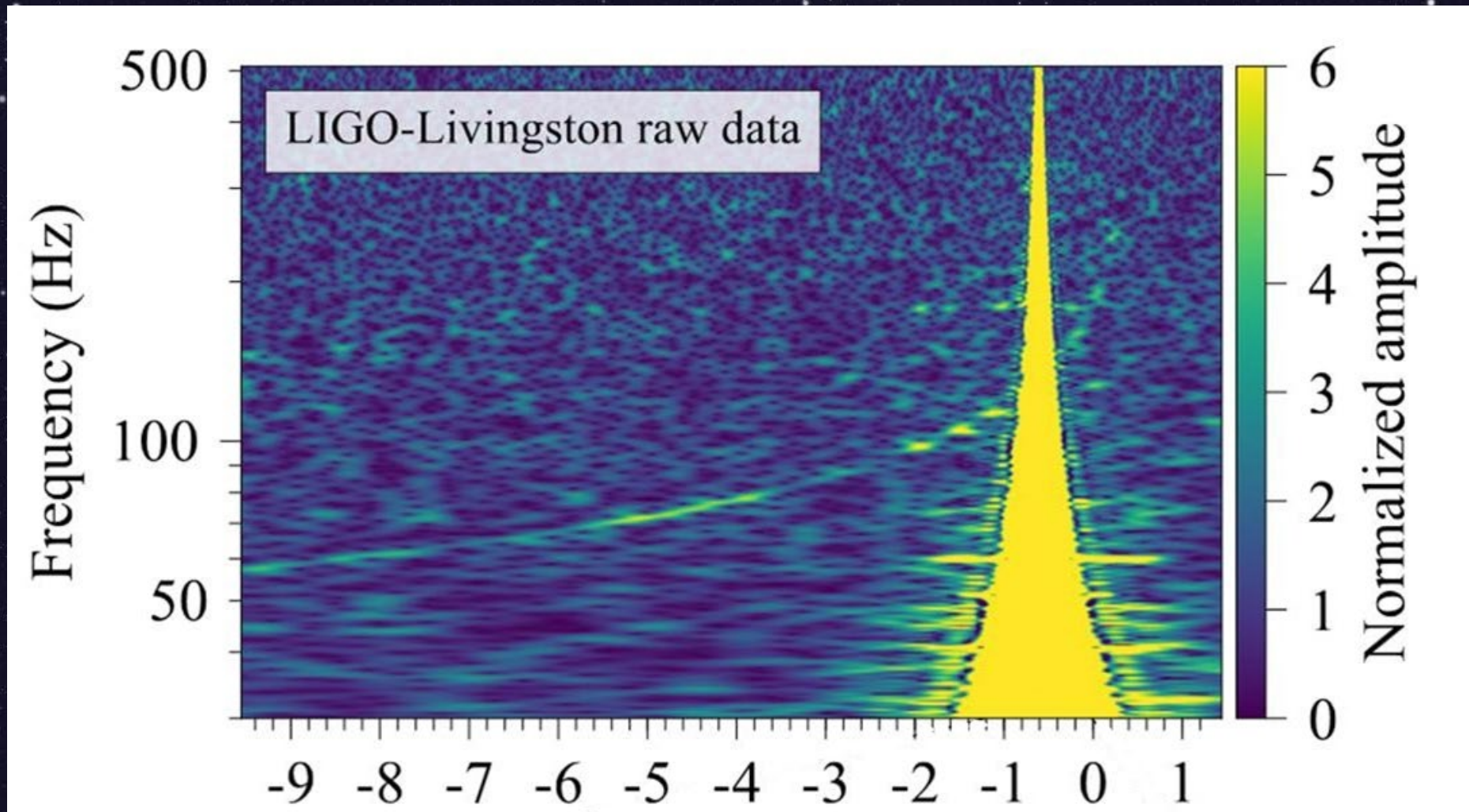


Fig 2, ApJL848, (2017) L13

# Binary Neutron Star Merger GW170817



Time (seconds) *Top of Fig 2 from LVC PRL119 (2017) 161101*

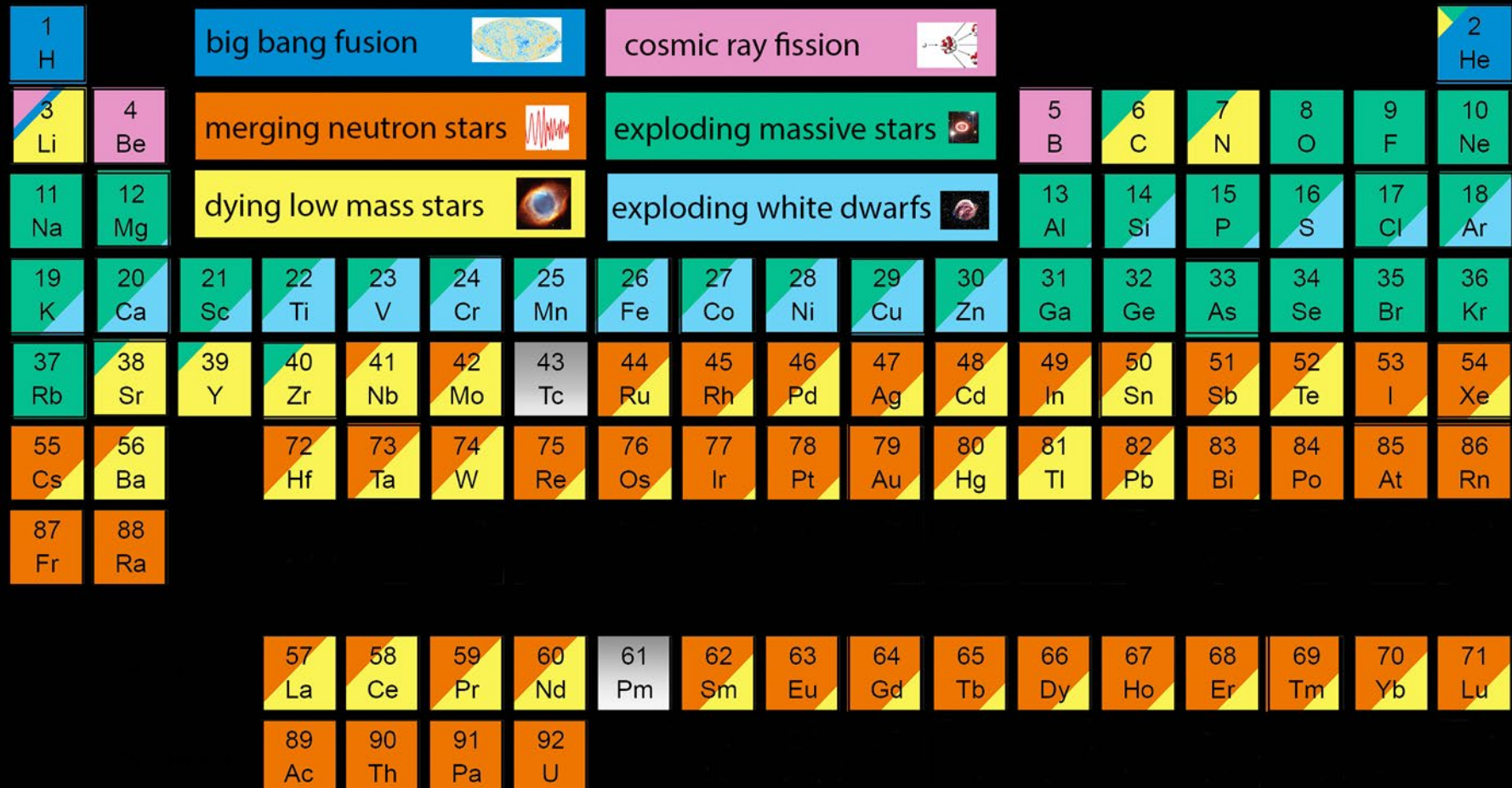
# BNS, short GRB

- Luminosity distance  $40^{+8}_{-14}$  Mpc, Fermi sGRB 1.7 sec later
- 2010 “realistic” rates projection 1000 per Gpc<sup>3</sup> per year, range 10 to 10,000
- Measured now to be  $1540^{+3200}_{-1220}$  per Gpc<sup>3</sup> per year
- Hubble constant  $70^{+12}_{-8}$  km per second per Mpc
  - Speed of gravity  $-3 \times 10^{-15} \leq \frac{\delta v}{v_{EM}} \leq 7 \times 10^{-16}$

*LVC PRL 119 (2017) 161101*

*LVC ApJL 848 (2017) L13*

# The Origin of the Solar System Elements



Astronomical Image Credits:  
ESA/NASA/AASNova

Graphic created by Jennifer Johnson

# Neutron star equation of state

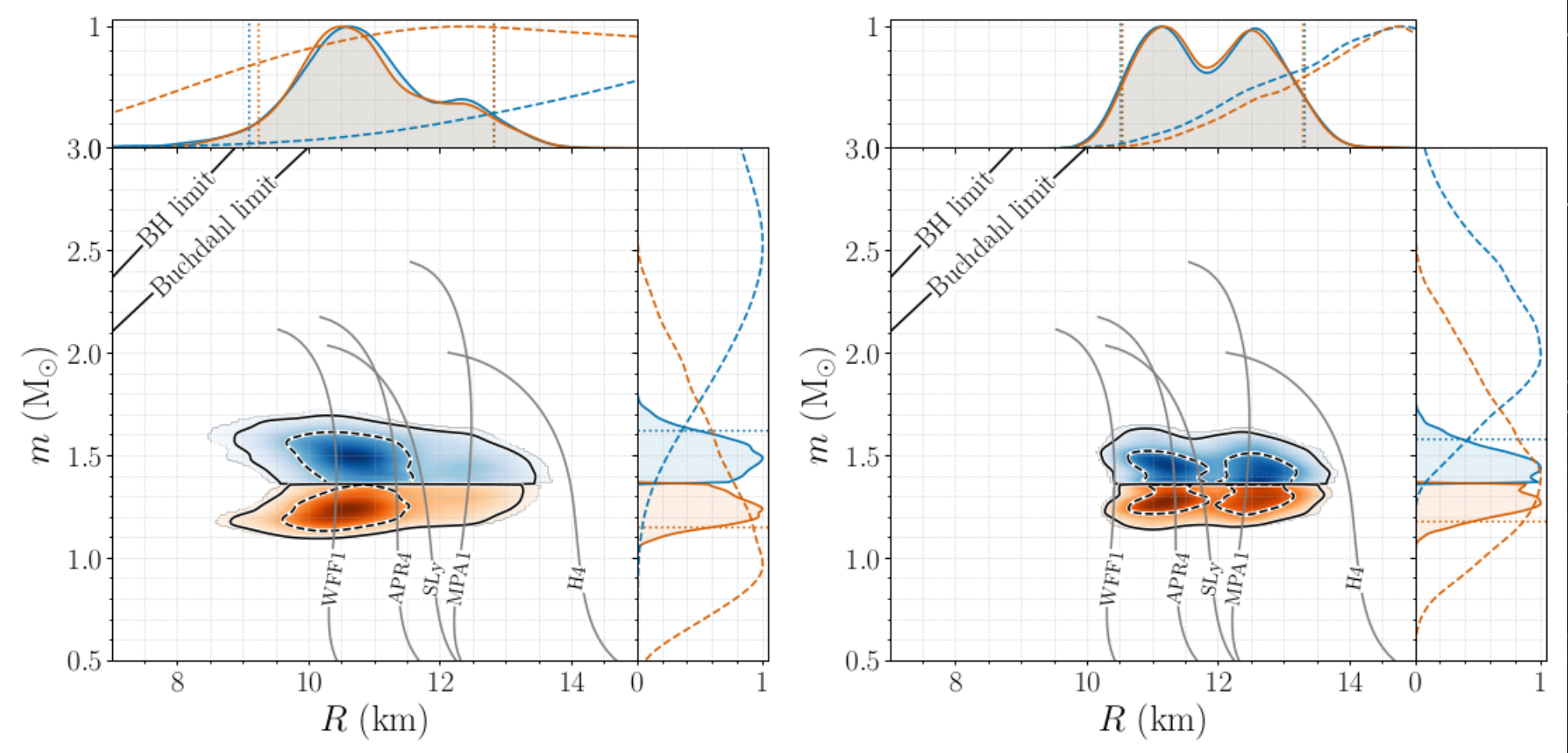
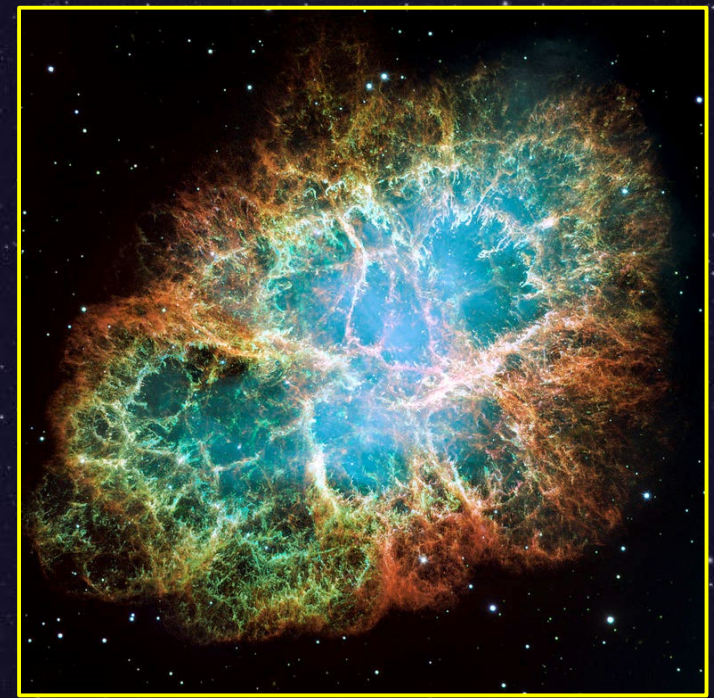


Fig 3 of “*GW170817: Measurements of neutron star radii and equation of state*” LVC arXiv: 1805.11581

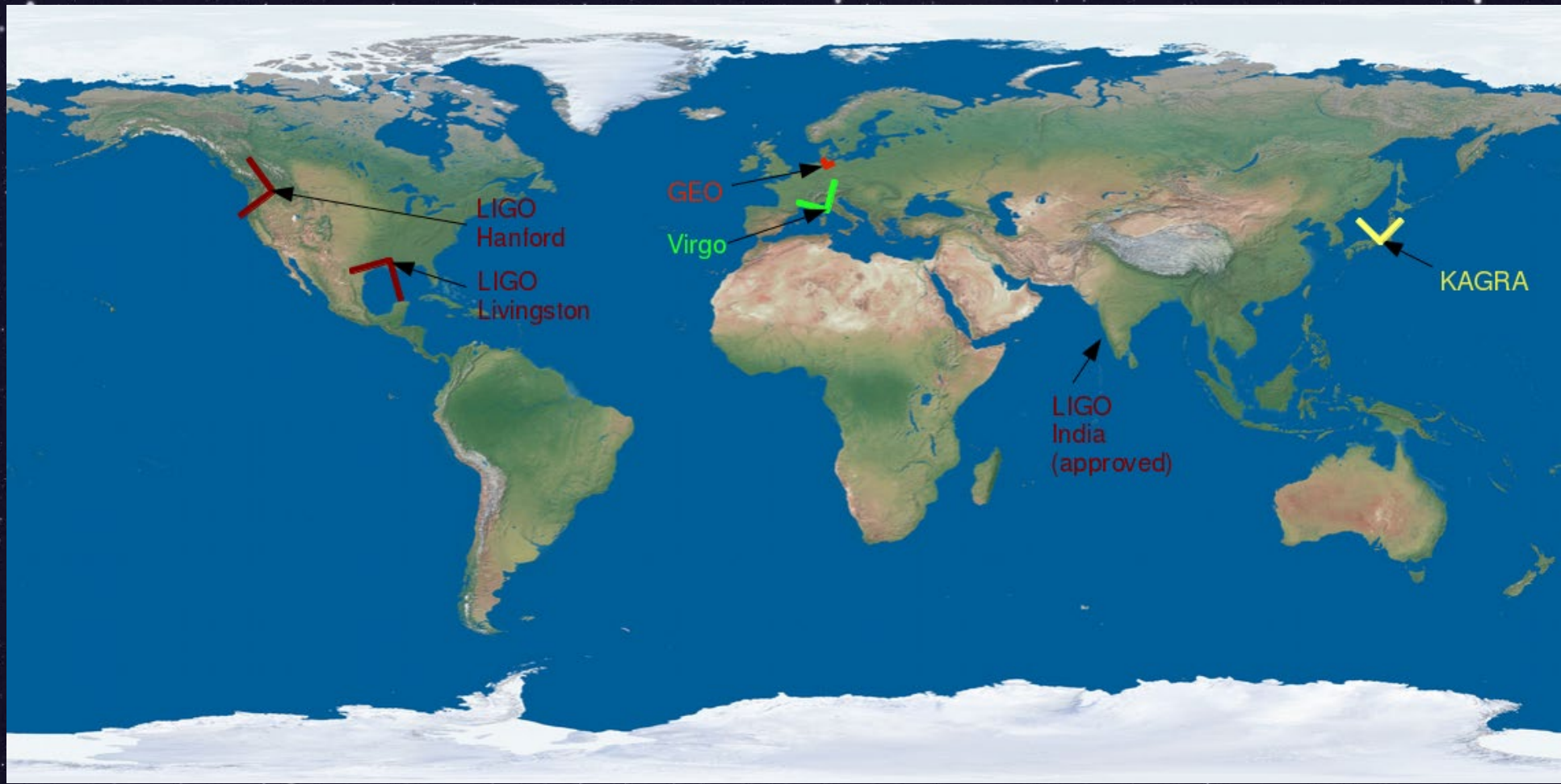
# Other potential GW sources

- Neutron star – Black hole systems *observed 2019! – awaiting details...*
- Deformed rotating neutron stars
- Galactic supernovae
- Intermediate-mass black holes
- Astrophysical background
- Cosmic strings
- First-order phase transitions
- Inflationary particle production
- Non-perturbative preheating
- Inflationary vacuum fluctuations



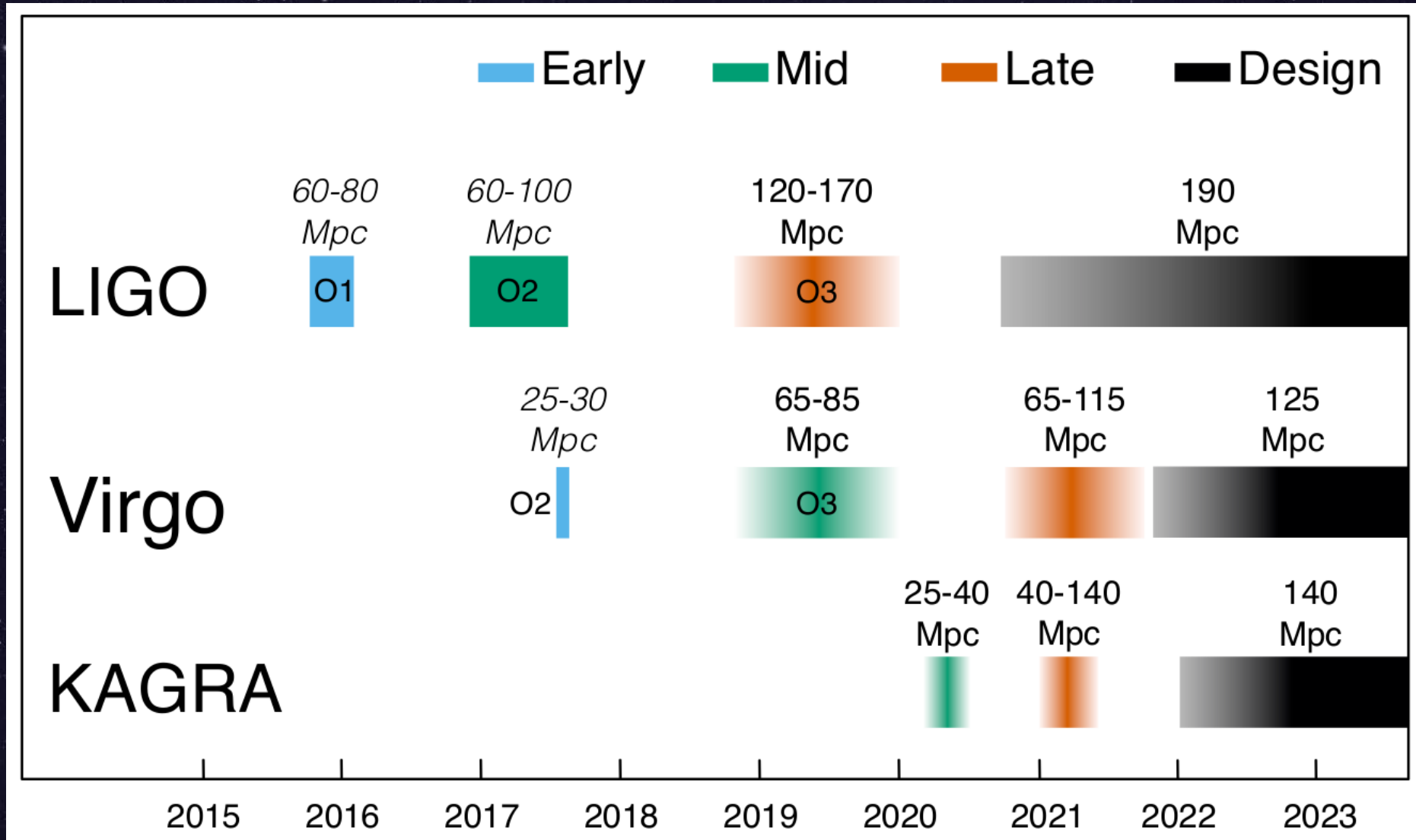
*Source: NASA/HST*

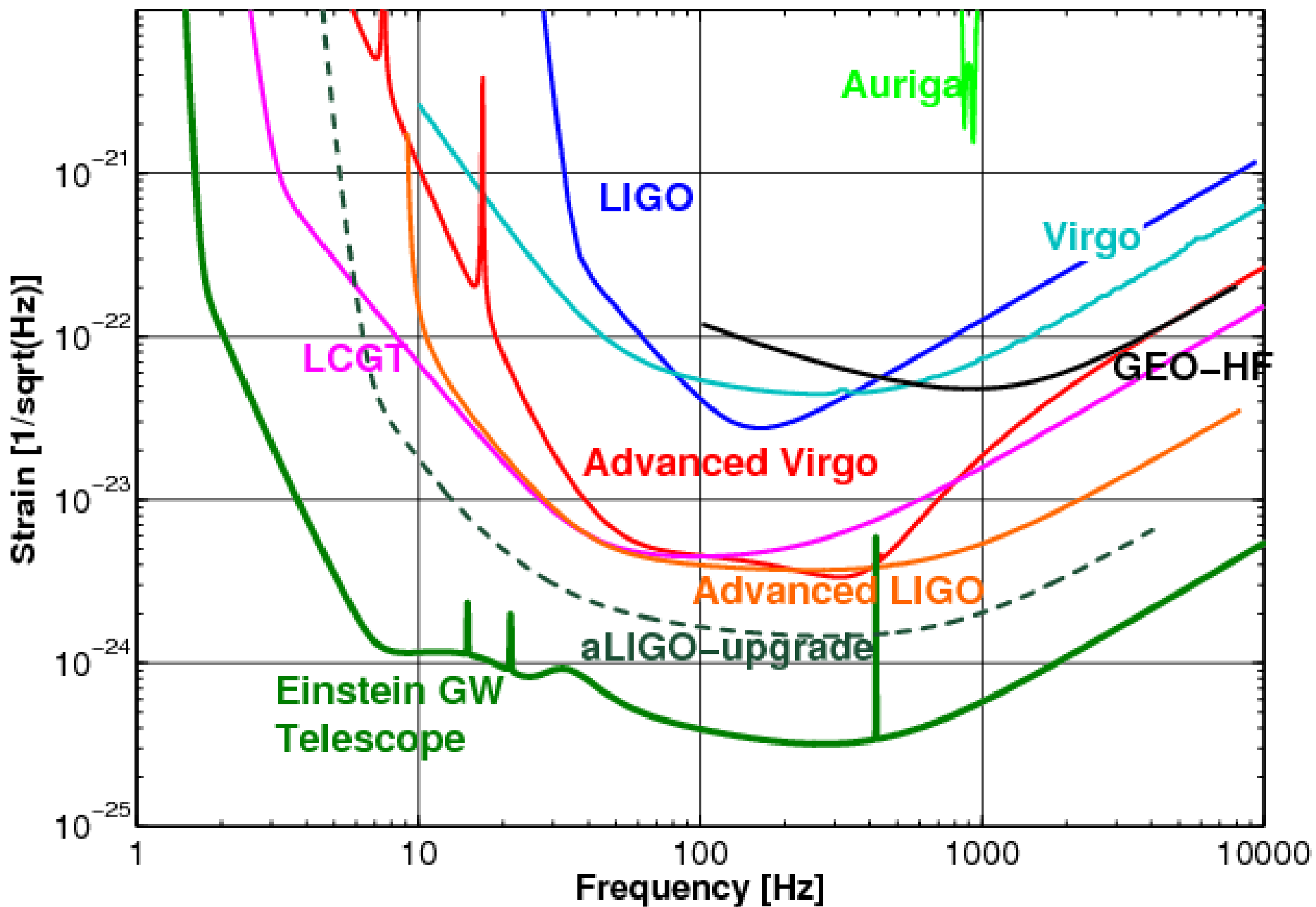
# Worldwide network



Source: Virgo/LAPP, T. Patterson

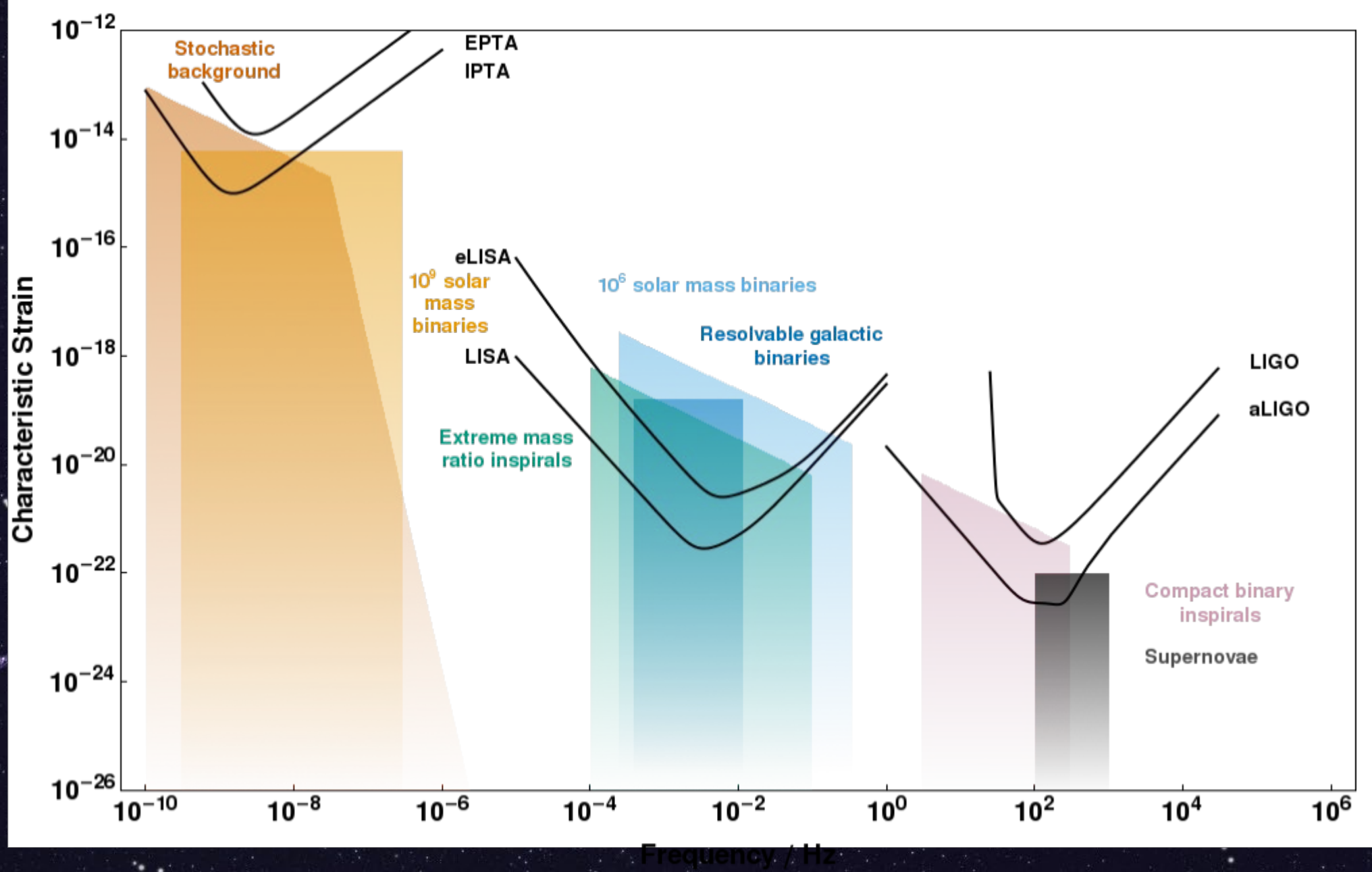
# Observing scenarios





Source: S. Hild (2012)

# Full GW spectra



Source: Wikimedia; C. Moore, R. Cole and C. Berry

# Reference resources

Abbott et al. “*The basic physics of the binary black hole merger GW150914*” arXiv:1608.01940, Annalen Phys. (2016) 041015

LIGO Open Science Center: <https://losc.ligo.org>

Science summaries: <https://www.ligo.org/science/outreach.php>

<https://www.zooniverse.org/projects/zooniverse/gravity-spy>

---

Data analysis software: <https://wiki.ligo.org/DASWG/LALSuite>

Data processing software: <https://gwpy.github.io/>

Papers: <https://www.lsc-group.phys.uwm.edu/ppcomm/Papers.html>

PyCBC (Template searches and significance): <https://pycbc.org/>

cWB (Umodeled search):

<https://www.atlas.aei.uni-hannover.de/~waveburst/LSC/doc/cwb/man/>

Thank you

# FERMI GBM OBSERVATIONS OF LIGO GRAVITATIONAL-WAVE EVENT GW150914

V. Connaughton<sup>1</sup>, E. Burns<sup>2</sup>, A. Goldstein<sup>3,20</sup>, L. Blackburn<sup>4,5</sup> , M. S. Briggs<sup>6,7</sup>, B.-B. Zhang<sup>7,8</sup>, J. Camp<sup>9</sup>, N. Christensen<sup>10</sup>, C. M. Hui<sup>3</sup>, P. Jenke<sup>7</sup> [+ Show full author list](#)

Published 2016 July 13 • © 2016. The American Astronomical Society. All rights reserved.

[The Astrophysical Journal Letters, Volume 826, Number 1](#)

## Abstract

With an instantaneous view of 70% of the sky, the *Fermi* Gamma-ray Burst Monitor (GBM) is an excellent partner in the search for electromagnetic counterparts to gravitational-wave (GW) events. GBM observations at the time of the Laser Interferometer Gravitational-wave Observatory (LIGO) event GW150914 reveal the presence of a weak transient above 50 keV, 0.4 s after the GW event, with a false-alarm probability of 0.0022 ( $2.9\sigma$ ). This weak transient lasting 1 s was not detected by any other instrument and does not appear to be connected with other previously known astrophysical, solar, terrestrial, or magnetospheric activity. Its localization is ill-constrained but consistent with the direction of GW150914. The duration and spectrum of the transient event are consistent with a weak short gamma-ray burst (GRB) arriving at a large angle to the direction in which *Fermi* was pointing where the GBM detector response is not optimal. If the GBM transient is associated with GW150914, then this electromagnetic signal from a stellar mass black hole binary merger is unexpected. We calculate a luminosity in hard X-ray emission between 1 keV and 10 MeV of  $1.8_{-1.0}^{+1.5} \times 10^{49}$  erg s<sup>-1</sup>. Future joint observations of GW events by LIGO/Virgo and *Fermi* GBM could reveal whether the weak transient reported here is a plausible counterpart to GW150914 or a chance coincidence, and will further probe the connection between compact binary mergers and short GRBs.

## Wider look at the gravitational-wave transients from GWTC-1 using an unmodeled reconstruction method

F. Salemi, E. Milotti, G. A. Prodi, G. Vedovato, C. Lazzaro, S. Tiwari, S. Vinciguerra, M. Drago, and S. Klimenko

Phys. Rev. D **100**, 042003 – Published 28 August 2019

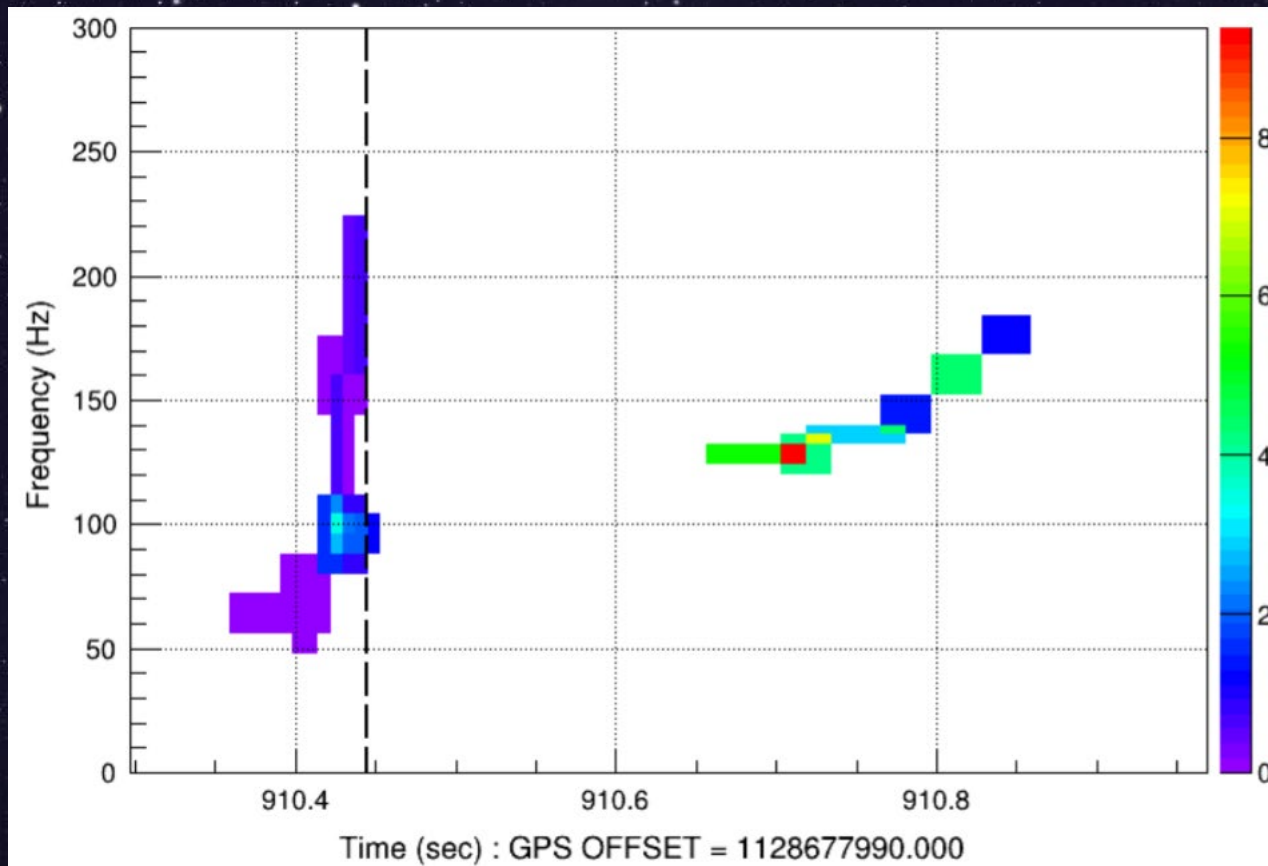


Fig 3d of Salemi et al, PRD100 (2019) 042003

## Parameter estimation and statistical significance of echoes following black hole signals in the first Advanced LIGO observing run

Alex B. Nielsen, Collin D. Capano, Ofek Birnholtz, and Julian Westerweck  
Phys. Rev. D **99**, 104012 – Published 7 May 2019

| Event     | Log Bayes factor | Max SNR |
|-----------|------------------|---------|
| GW150914  | -1.8056          | 2.86    |
| LVT151012 | 1.2499           | 5.5741  |
| GW151226  | 0.4186           | 4.07    |

TABLE II. Table of Bayes factor results. Negative values indicate that the Gaussian noise hypothesis is preferred. Positive values indicate that the echoes hypothesis is preferred after marginalization over parameters. Log Bayes values with magnitude  $< 1$  are “not worth more than a bare mention” in the nomenclature of [43].

# X-ray binaries masses and spin

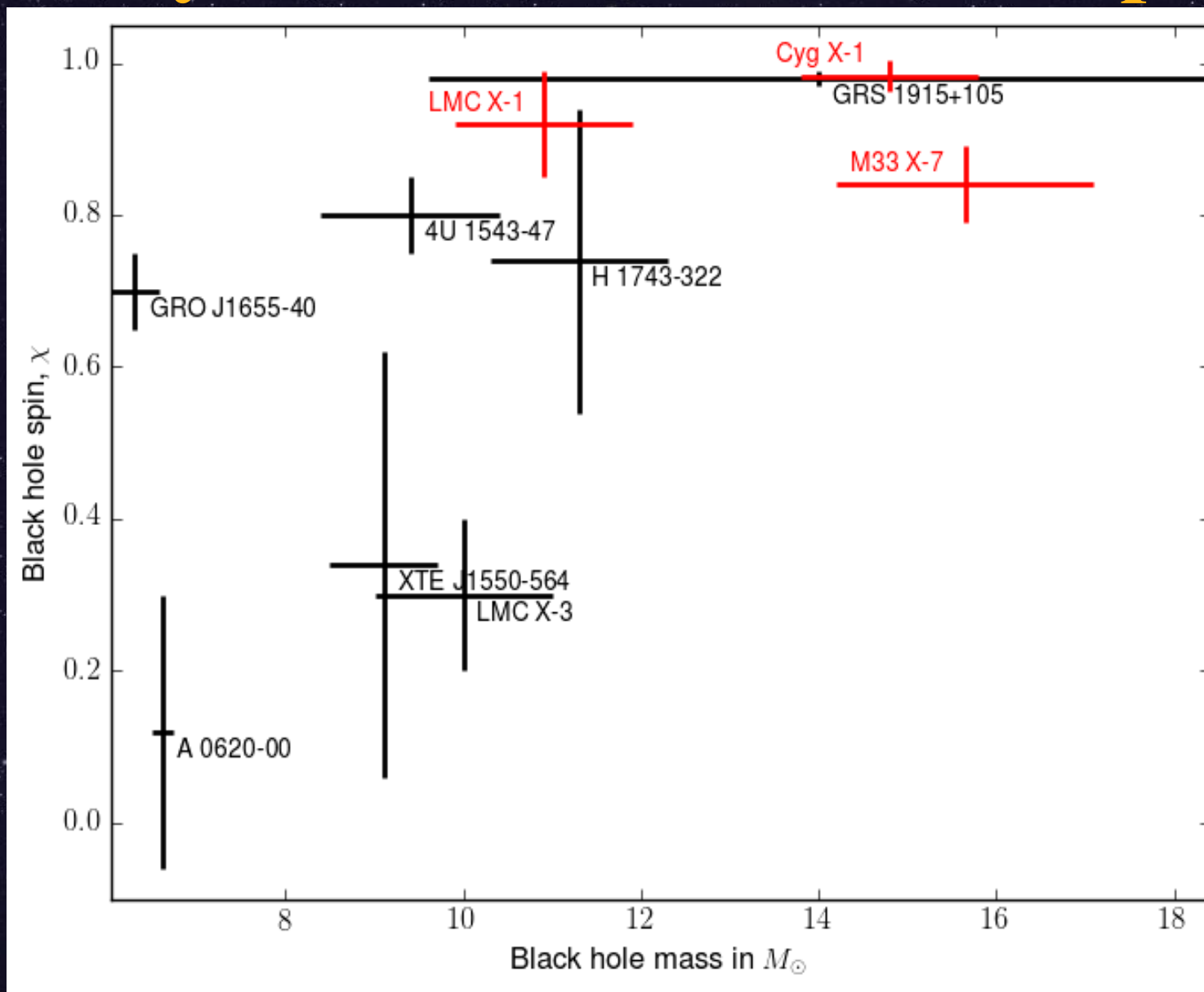
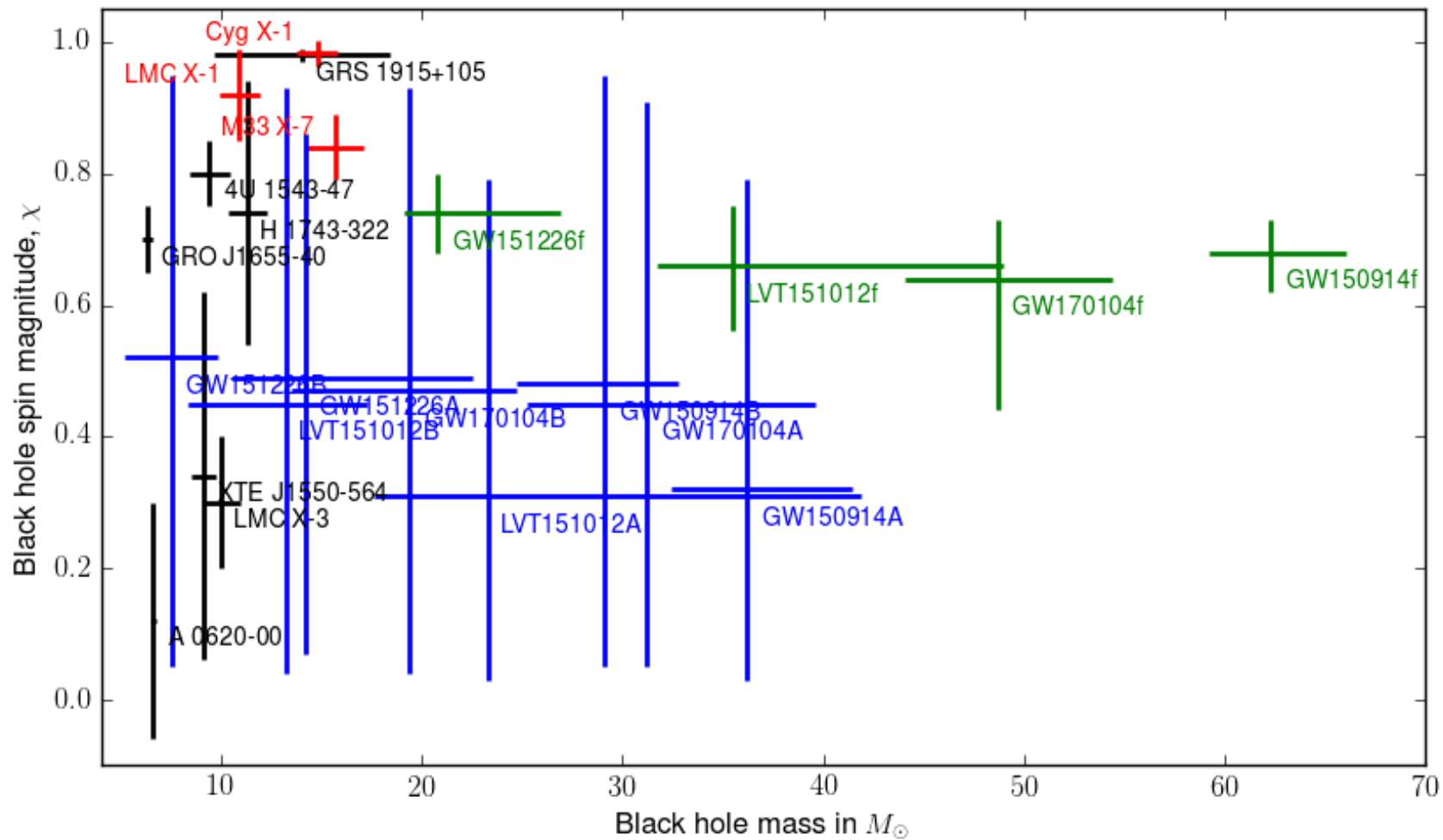
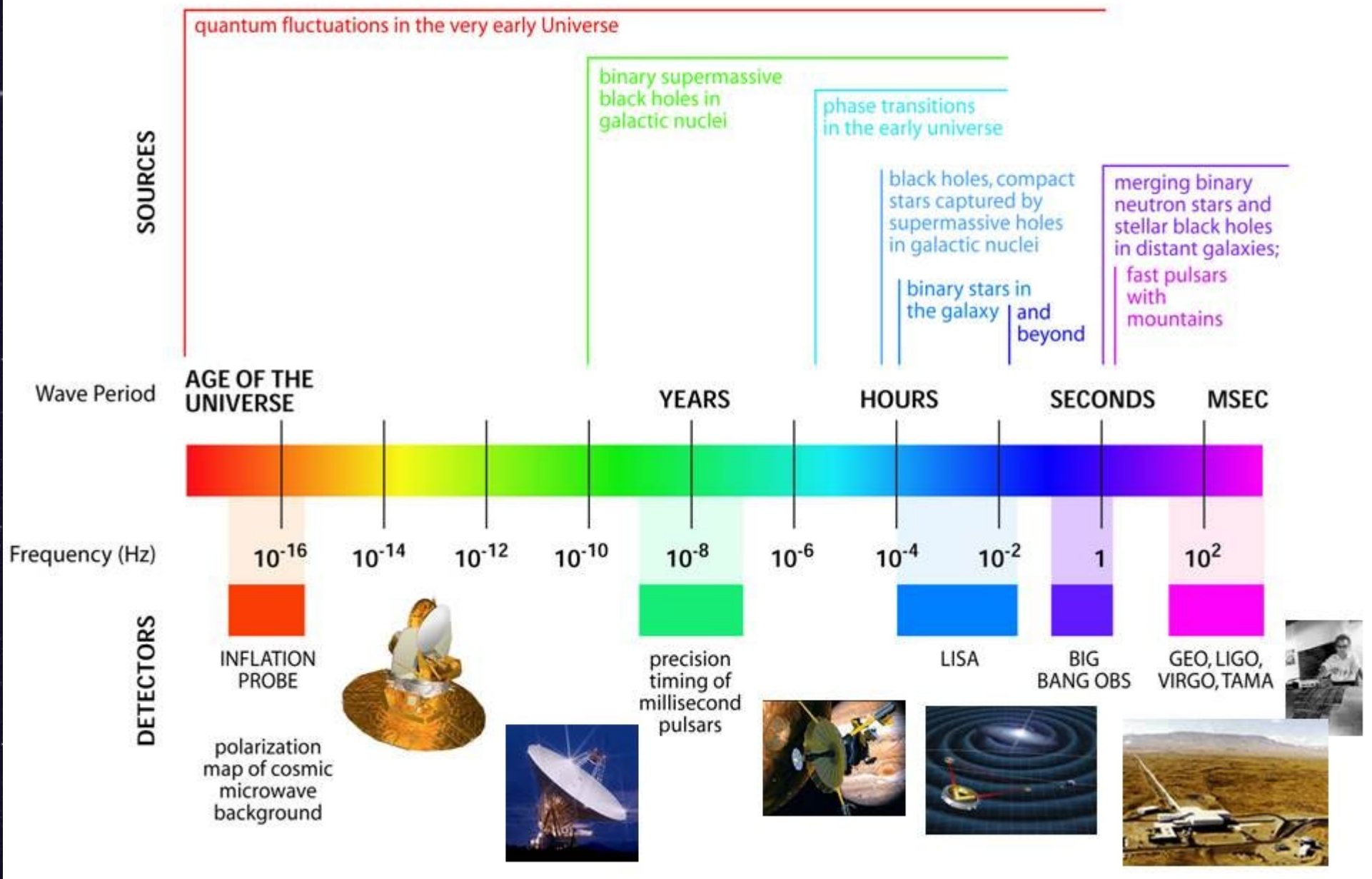


Fig. 1 of Nielsen J.Phys.Conf.Ser. 716 (2016) no.1, 012002

# X-ray + GW masses and spins



# THE GRAVITATIONAL WAVE SPECTRUM



Source: Martin Hendry